Correlation Between Strand Stability and Magnet Performance

D. R. Dietderich, S. E. Bartlett, S. Caspi, P. Ferracin, S. A. Gourlay, H. C. Higley, A. F. Lietzke, S. Mattafirri, A. D. McInturff, G. L. Sabbi, and R. M. Scanlan

***Abstract*—Magnet programs at BNL, LBNL and FNAL have observed instabilities in high J_c Nb_3Sn strands and magnets made from these strands. This paper correlates the strand stability determined from a short sample-strand test to the observed magnet performance. It has been observed that strands that carry high currents at high fields (greater than 10 T) cannot sustain these same currents at low fields (1–3 T) when the sample current is fixed and the magnetic field is ramped. This suggests that the present generation of strand is susceptible to flux jumps (FJ). To prevent flux jumps from limiting stand performance, one must accommodate the energy released during a flux jump. To better understand FJ this work has focused on wire with a given sub-element diameter and shows that one can significantly improve stability by increasing the copper conductivity (higher residual resistivity ratio, RRR, of the Cu). This increased stability significantly improves the conductor performance and permits it to carry more current.**

***Index Terms*—Critical current, flux jumps, magnet, Nb_3Sn, RRR, stability.**

I. Introduction

THE Superconducting Magnet Group of Lawrence Berkeley National Laboratory has fabricated several high field magnets from Nb_3Sn. Most of the magnets, both full-scale (RD-3b, RD-3c and HD-1) and sub-scale (SM-01, SM-04, and SM-05), achieved greater than 90% of the short sample current [1]–[8]. However, several subscale magnets with different conductor and different magnetic fields only achieved 40–70% of their short sample limit calculated from strand measurements (Table I). Similar behavior has been observed in magnets at Fermi National Accelerator Laboratory (FNAL) [9]. Strand and cable measurements made at FNAL and Brookhaven National Laboratory suggest that the conductor is unstable [10]–[13] with stability being defined as the ability to reach the critical current of the conductor. It has been postulated that flux jumps in the low field regions of the magnets are the origin of the poor magnet performance [14]. However, critical current measurements showed that the strands could sustain high currents, well above the magnet current limit. The magnet performance could not be explained by the strand data.

II. Magnet Performance

Test results from prototype magnets fabricated using SM-type subscale coils have prompted a study of strand stability. Two of these recently tested prototypes (SM-06 and NMR-1) were limited to quench currents well below their calculated short sample limits (Table I). The SM-06 diagnostics showed voltage imbalances consistent with flux-jumping behavior in the low field region preceding the magnet quenches. The limiting coils (SC-12 in NMR-1 and SC-13 in SM-06) were made with the same Modified Jellyroll strand (ORe 186, seen in Fig. 1(a)) and were reacted together. The final step of the multi-step heat treatment was 650°C for 72 h. Even with this short heat treatment time, the RRR (ratio of the resistance at 300 K to that at 20 K) of the two coils was low, in the range of 7-12. The low RRR is believed to result from a rapid conversion of the Nb barrier to Nb_3Sn, thus permitting Sn to diffuse into the Cu stabilizer.

Another MJR strand (ORe 143, seen in Fig. 1(b)) whose properties were much less sensitive to heat treatment conditions, could be given a final heat treatment of 650°C for 180 h and provide higher RRR values, in the range of 37–42. This strand has been used in magnets (SM-01 [6] and SM-04 [7]) that reached their short sample limit. These magnets were assembled from coils SC-01, SC-02 and SC-08, all of which performed very well. Coils SC-01 and SC-02 formed the first sub-scale magnet, SM-01, of the racetrack design. As can be seen in Table I these

TABLE I
Magnet and Coil Characteristics

Magnet	SC-Coil	Strand in Coils	RRR Coil (Strand)	FJ Stability[a]	I_{mag}[b] (A)	I_{mag}/I_{ss}
SM-01	01	ORe143	36	S	496	1.0
	02	ORe143	42	S		
SM-02	02	ORe143	42	S		
	03[c]	EP 214	226 (125)	U	288	0.4
SM-03	01	ORe143	36	S		
	06[d]	ORe143	167 (36)	U	436	0.7
SM-04	01	ORe143	36	S	489	1.0
	08	ORe143	42	S		
SM-06	13	ORe186	7	U	338	0.6
	14	ORe186	12	?		
NMR-1	01	ORe143	36	S		
	02	ORe143	42	S		
	11	ORe186	8	?		
	12	ORe186	7	?	324	0.6
SQ-01	01	ORe143	36	S		
	02	ORe143	42	S		
	15[e]	RRP6555	99	S		
	16[e]	RRP6555	87	S	532	0.9

[a] Definition of notation: S, stable; ?, unknown; U, unstable.
[b] This is the current carried per strand. The peak magnet current has been normalized to the number of superconducting strands in the cable.
[c] This coil had several issues: Mechanically unstable cable with "out of pattern" strands during winding and voids in the epoxy from incomplete impregnation.
[d] At least 7 of the 14 superconducting strands were broken about 10 mm from the lead splice.
[e] Magnet was limited by coils SC-16 due to conductor motion. Flux jumps were observed at low fields during the ramp but did not appear to limit coils.

Manuscript received October 5, 2004. This work was supported by the U.S. Department of Energy under Contract DE-AC02-05CH11231.

The authors are with the Lawrence Berkeley National Laboratory, Berkeley, CA 94720 USA (e-mail: drdietderich@lbl.gov).

Digital Object Identifier 10.1109/TASC.2005.849155

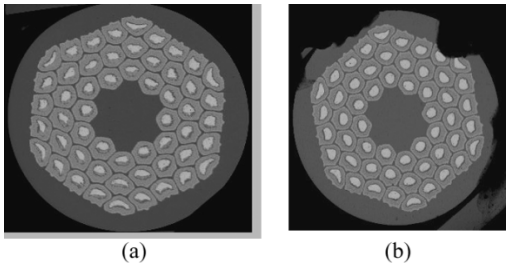

Fig. 1. SEM micrographs of the strands before heat treatment. Both wires have a diameter of 0.7 mm. (a) Strand ORe 186. (b) Strand ORe 143. The black regions around the circumference of the wire are carbon paint for electron microscopy.

coils have been paired with other coils for several magnet tests. These two coils when used in several different magnet configurations since SM-01 have always performed as expected. The strand (ORe 143) in these coils is stable.

The stability of strand ORe 143 was demonstrated in coil SC-08. Magnet SM-04 was made in collaboration with FNAL using a new ceramic insulation scheme (all of the LBNL coils used S2-glass insulation) to test if such an insulation system had an impact on magnet performance. The magnet went to its short sample current limit thus showing that the ceramic insulation system did not affect the strand behavior or the magnet performance [7].

Two other SM-series magnets (SM-02 and SM-03) that did not perform as expected had various issues from mechanically unstable cable which caused strands to be displaced completely out of the Rutherford cable pattern or voids in the epoxy (coil SC-03), or broken strands in a lead (coil SC-06) [15]–[17]. In addition, both of these coils were made with a cable that was a mixture of superconducting and Cu strands. This made the interpretation of the test results and magnet performance difficult. Was it a problem with the wire, the mixed-strand character of the cable, or voids in the epoxy? Even with these issues the magnet performance may provide some insight into magnet stability. This will be discussed later.

Strands ORe 186 and ORe 143 of the SM-series magnets are practically identical in terms of wire diameter (0.7 mm), sub-element diameter $(\mathrm{D_{eff}})$, number of sub-elements (54) and Cu fraction ($\sim$50%). Cross sections of the wires are shown in Fig. 1. As a result, it should be possible to obtain comparable performance from both strands. This work is a study of one parameter, the RRR (i.e. residual resistivity) on stability. The first sub-scale magnet (SM-01) made from ORe 143 wire went to 99% of the short sample current of 500 A per strand. The main difference between the two strands is the low RRR of the coils with strand 186. This seems to be due to the diffusion barrier of ORe 186 reacting faster than that of ORe 143, thus contaminating the Cu stabilizer with Sn. If strand ORe 186 is heat-treat so that its RRR is nearly the same as that of ORe 143 then it should also be stable. The experimental results that follow confirm this.

III. Strand Stability

To understand the behavior of a superconducting (SC) magnet one must consider the behavior at each level, i.e. filament, sub-element, strand, and cable, as well as the glass insulation, and epoxy. This work focuses on stability at the strand level. The stability relationship between RRR, $\mathrm{J_c}$ and filament size has been known for many years; to dynamically stabilize NbTi conductor the filament diameter needed to small, about 10 $\mu\mathrm{m}$ or less [18]. With $\mathrm{Nb_3Sn}$'s higher $\mathrm{T_c}$ a smaller change in critical current with temperature results in greater stability. This provides more temperature margin than can be achieved with NbTi since it only has a Tc of $\sim$10 K. Plus as the temperature increases from 4.2 K both the heat capacity and thermal conductivity of the stabilizing Cu increases. Until recently low field instabilities had not been an issue with $\mathrm{Nb_3Sn}$ wire, but with the present generation of conductor with large sub-elements (greater than 100 $\mu\mathrm{m}$) and critical currents over 2500 $\mathrm{A/mm^2}$ at 12 T and 4.2 K, flux jump (FJ) issues appear to have returned.

One of the first high-field superconducting materials available for magnet applications was $\mathrm{Nb_3Sn}$ tape. To dynamically stabilize it against FJ high purity copper (or aluminum) was co-wound or soldered to $\mathrm{Nb_3Sn}$ tape [19]. This work showed that an unstable tape, which has a large effective filament diameter $(\mathrm{D_{eff}})$ due to its large width (1.5–3 mm), could be made stable. The Cu serves at least three purposes: One, provide a current path when the superconductor goes normal. Two, provide heat capacity so that the SC can recover from the heat generated by a disturbance. Three, slow the motion of the FJ (Lentz's Law) and thus the heat generation rate, giving the SC time to thermally recover and return to the SC state. Four, is a high lambda to transport heat away from the superconductor. At 4 K the thermal conductivity of Cu increases by a factor of 2.5 as the RRR increases from 30 to 100; the increase is about an order of magnitude if the RRR rises to 300. A significant fraction of this improvement is maintained even in low magnetic field ($\sim$1 T) [20]. There is almost a linear increase of thermal conductivity of Cu with increasing RRR between 4–20 K. Both of these aspects of Cu, higher thermal conductivity and higher electrical conductivity, aid in improving strand stability.

IV. Sample Preparation and Measurements

All of the samples were heat-treated in a flowing argon atmosphere during the entire thermal cycle. The samples were all heat treated and tested on Ti-alloy barrels. Titanium alloy end rings used during the heat treatment were removed to mount the barrel onto the test holder. All of the samples were bonded to the barrel with a thin layer of Stycast epoxy at the fillet between the wire and the groove of the barrel. The top surface of the strand was exposed to the liquid helium bath. An extra $\mathrm{Nb_3Sn}$ jumper wire is added across the transition between the Cu holder and the Ti barrel. The jumper is about 1.5 turns in length (with 3/4 of a turn on the Cu and 3/4 of a turn on barrel) in parallel with the sample.

The magnetic field sweep rate for strand experiments was chosen to match the low-field ramp-rate (20–25 mT/s) given to LBNL's SM-type magnets. Several field sweeps are performed while increasing the sample current until a threshold is reached such that the sample quenches. The stability current $(\mathrm{I_s})$ is defined as the highest current that the sample can carry without quenching while the field is ramped up or down. The wire still shows FJ behavior below $\mathrm{I_s}$ during the field ramp but the magnitude of the FJ is small enough that the sample can recover.

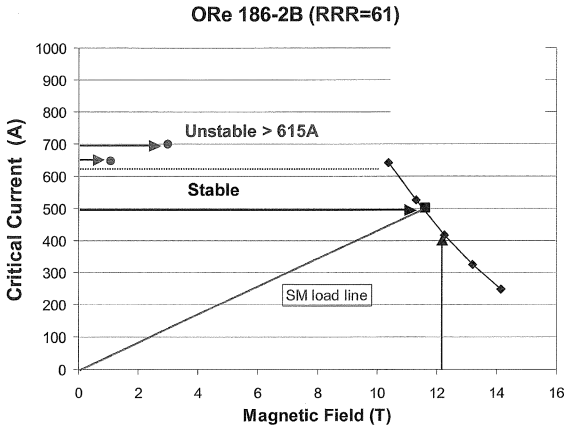

Fig. 2. Critical current vs. magnetic field for strand ORe 186 with an RRR of 61. The strand is stable to above 615 A. With the current fixed at 500 A the field can be ramped to the short sample $I_c(H)$, the square data point.

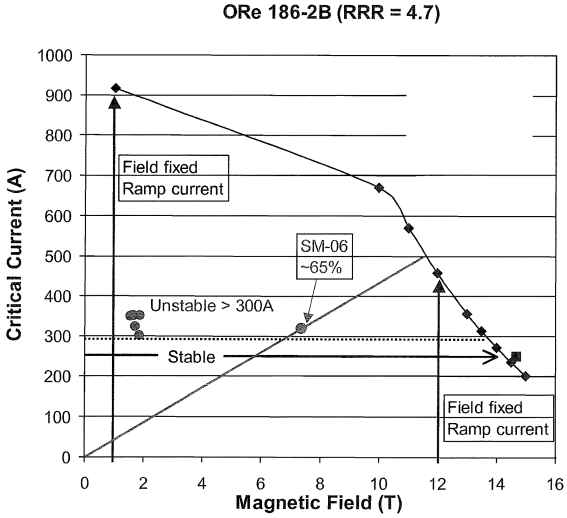

Fig. 3. Critical current vs. magnetic field for strand ORe 186 with an RRR of 4.7. The strand is only stable to about 300 A. With the current fixed at 250 A the field can be ramped to the short sample $I_c(H)$, the square data point. The load line of SM-06 is included in the figure. The peak strand current in the magnet is the round data point on the line at 65% of predicted short sample limit.

For measurements of I_c at high fields the magnetic field was fixed and the current was ramped from zero to the transition from a V(I) curve. A 10 micro-V/m criterion was used for I_c determination. Below I_s the critical current could also be obtained by ramping the field and obtaining a V(H) curve.

V. Strand Performance

By heat-treating samples of ORe 186 for different times at the same temperature, wires with similar critical currents but very different RRR values (between 61 and 4.7) were obtained. A possible approach, which simulates magnet operation, is to test strand for a low-field instability by fixing the sample current and sweeping the field. With this procedure, the higher RRR sample could sustain currents greater than 600 A (Fig. 2), while the sample with the lower RRR quenched at currents a factor of 2 lower (∼300 A, Fig. 3). The horizontal dashed line represents the highest current that the sample could carry and remain stable (I_s). There were a few field sweeps for which the sample was

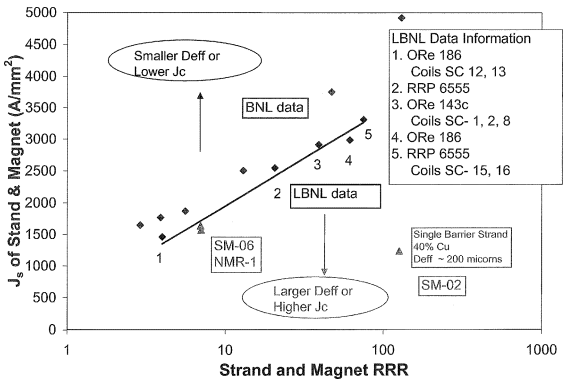

Fig. 4. The critical stability current density (Js) of strands and magnets as a function of the strand and magnet RRR. Note that the graph is a semi-log plot.

stable above I_s. However, I_s has been defined as the highest current at which no quenches occur.

The load line for SM-06 is included in Fig. 3. The highest quench current (338 A per strand) is shown on the load line. All of the other quenches were below this, but not by more than 5%. There is a well-defined quench level, or threshold, in the magnet that is also seen in the wire. For sample currents below I_s the field can be ramped to the short sample limit providing a V-H curve. This is shown as a solid horizontal line with an arrowhead that ends at I_c (data points denoted with square symbols).

At high fields the critical current of the sample could be measured for currents well above I_s by fixing the field and ramping the current. At 10 T the I_c is almost 700 A. However, at lower field the strand is unstable. When the field is fixed at 1 T and the current is ramped, the sample quenches at ∼900 A (Fig. 3). At this time it is not clear if the sample is unstable at high currents and low fields or if there is a problem with the present measurement methods and sample mounting techniques given in [21], the international testing standard for DC current measurement of Nb_3Sn conductors. The sample is also unstable when the current is fixed above 300 A and the field is ramped. However, this quench current is well below 900 A. Both of these procedures show that the strand is unstable.

When the heat treatment time of the sample is decreased to obtain a higher RRR of 61 there is an increase in the strand stability (Fig. 2). For this RRR the strand is stable above 600 A. This is well above the short sample limit for magnet SM-06. At 12 T (no self-field correction) and 4.2 K the I_c is 417 A. The shortened heat treatment time reduced the wire I_c (12 T, 4.2 K) by ∼10% but it is a beneficial tradeoff to obtain a stable conductor and magnet.

Our group's first short Nb_3Sn quadrupole magnet (SQ-01), made from 4 racetrack coils, did not reach its short sample current limit. At this time it is not clear why the magnet performance was limited by coils SC-15 or SC-16, since they did not show instability-driven quenches up to the maximum achieved current of 530 A/strand and their short sample current limit was higher than the baseline coils SC-01 and SC-02. Performance can be limited by problems other than stability.

Fig. 4 plots log J_s of ORe 186, ORe 143, and RRP 6555 as a function of RRR. The plot includes shows a consistent behavior for all the strands, J_s increase with increasing RRR. The data also shows that for RRR's of 40 or greater the strand seems to

be stable at 600 A and above. The strand that produced each data point is noted in the figure along with the coils fabricated from that stand. The plot also includes data from [11] that will be discussed later.

VI. Discussion

The results presented here help to explain some of the poor performing magnets at LBNL and perhaps at FNAL. Most, if not all of the magnets that only achieved 40–70% of short sample had low RRR's in the range of 5–7. Two magnets tests, SM-06 and NMR-1 at LBNL, had coils with RRR's of 7. The performance of these two magnets is shown in Fig. 4 as triangle data points and given in Table I. It shows that the highest stable current (I_s) in the magnet is once again consistent with the strand data.

Another magnet (SM-03) that performed poorly was made with coil SC-06. The coil was made with a mixed strand cable consisting of 14 strands of ORe 143 and 7 Cu strands. It did not reach its calculated short sample limit. The magnet performed badly due to at least 7 of the 14 superconducting strands being broken near the lead splice. The crack pattern across the cable suggests that it was subjected to a hard-way bend after reaction.

Even though coil SC-06 was damaged it can provide insight into strand and magnet stability. With the peak current in magnet SM-03 being in the range 5761 to 6104 A the seven good strands had to each carry 823 to 873 A. This shifts the current per strand up into the unstable region shown in Fig. 5. Analysis of quench initiation data in coil SC-06 suggests that FJ preceded the magnet quench. This shows that we are pushing the limit of strand stability but it also suggests that the magnet may have performed as designed if there were no broken strands.

Additional studies of strand stability have been reported in [11]. The strand used in [11] was the same RRP 6555 strand used in part of this work, although from a different section of the billet. If the data of [11] is included along with LBNL's data in a semi-log plot of J_s vs. RRR it is seen that data of LBNL has a linear fit (Fig. 4). The reason for this is not clear. The BNL data is similar to the LBNL data in the low RRR range but diverges at higher RRR. The reason for the difference between the two sets of data is not understood at this time.

Also included in Fig. 4 is the quench current per strand of magnet SM-02. One coil of this magnet was made with a mixed strand cable (14 superconducting strands and 7 Cu strands) as discussed before. The superconducting strand EP 214, made by IGC, consisted of 19 sub-elements inside a single diffusion barrier. The diameter of the barrier (non-Cu area) was ∼500 microns. However, with the sub-elements being internally split the magnetically measured D_{eff} was ∼195 microns [22]. Even with the strands high RRR of 126, its J_s is low, consistent with its large D_{eff}. This was the only magnet fabricated at LBNL using this type of strand.

The stability of another strand (ORe 021) not reported here but presented in [23] shows that a wire with comparable Cu fraction and the same internal geometry (54 sub-elements distributed in three rings) but a smaller sub-element diameter is stable at low field. This shows the importance of decreasing the sub-element size in the type of conductor.

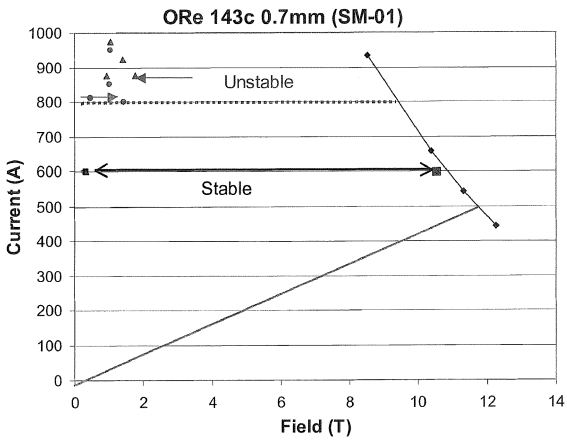

Fig. 5. The I_c as vs. magnetic field (high field data) for strand ORe 143 that was in the baseline coils SC-01 and SC-02. The stand is unstable at 800 A an above but it is stable at 600 A and below. The I_s limit is between these two values.

If one assumes the energy in a flux jump is proportional to the product $J_c^2 \times D_{eff}^2$, with D_{eff} being the effective filament size, then some predictions can be made regarding strand and magnet performance. The energy in the FJ heats the surrounding material and the temperature increases. The temperature increase depends on the heat capacity of the SC, bronze and Cu stabilizer and the thermal conductivity of the Cu. If the RRR of the Cu stabilizer is low then little heat can be removed in the time required for the SC to revert back to the SC state. All of the heat must be accommodated by the heat capacity of the material.

The results of this work suggest that the two magnets (SM-06 and NMR-1) may have performed as expected reaching their short sample current limit if the RRR was increased to about 40. In the near future, new coils and SM-type magnets will be made and tested with the same ORe 186 strand. However, the coils will be heat treated to obtain a higher RRR to confirm this hypotheses or not.

VII. Conclusions

This work shows that for a given wire diameter, subelement size (D_{eff}), and Cu fraction, the RRR of the strand determines the low field instability current limit I_s. Although this effect can be inferred from the relations developed by Wilson and others it has only appeared as a practical problem in the new high J_c, large sub-element strand that has been developed for the High Energy Physics magnet programs. Since all of the filaments within a sub-element sinter during the Nb_3Sn formation producing a large "effective filament" the only means to assure strand stability is to reduce the sub-element size from present levels. The different sub-element designs (single barrier vs. multiple barrier) appear to have an impact on stability. However, the results presented show the importance of retaining a high RRR, even if one must make the tradeoff of reducing J_c slightly at high fields, to insure strand and magnet stability.

References

[1] A. F. Lietzke *et al.*, "Fabrication and test results of a high field Nb_3Sn racetrack dipole," in *Proc. Part. Accel. Conf.*, Jun. 2001, p. 208.

[2] ——, "Test results of RD-3c, a Nb_3Sn common-coil racetrack dipole magnet," *IEEE Trans. Appl. Supercond.*, vol. 13, pp. 1292–1296, 2003.

[3] ——, "Test results for HD-1, a 16 Tesla Nb_3Sn dipole magnet," *IEEE Trans. Appl. Supercond.*, vol. 14, pp. 345–348, 2004.
[4] R. R. Hafalia *et al.*, "An approach for faster high field magnet technology development," *IEEE Trans. Appl. Supercond.*, vol. 13, pp. 1258–1261, Jun. 2003.
[5] L. Chiesa *et al.*, "Performance comparison of Nb_3Sn magnets at LBNL," *IEEE Trans. Appl. Supercond.*, vol. 13, pp. 1254–1257, 2003.
[6] M. Coccoli and L. Chiesa, "SM-01a and SM-01b Test Results,", LBNL-50145, SC-MAG #775, Feb. 2002.
[7] L. Chiesa *et al.*, "Test Results of Magnet SM-04,", LBNL SC-MAG. #795.
[8] L. Imbasciati *et al.*, "Study of the effects of high temperature during quenches on the performance of a small Nb3Sn racetrack magnet," presented at the 6th Eur. Conf. Appl. Supercond., Sorrento, Italy, Sep. 14–18, 2003.
[9] S. Feher *et al.*, "Test results of shell-type Nb_3Sn dipole coils," *IEEE Trans. Appl. Supercond.*, vol. 14, pp. 349–353, Jun. 2004.
[10] E. Barzi, "Instabilities in transport current and magnetization measurements of Nb_3Sn and NbTi strands," in *Presentation at Workshop on Instabilities in* Nb_3Sn *Strands, Cables, and Magnets, FNAL*, Apr. 28–30, 2004.
[11] A. K. Ghosh *et al.*, "Dynamic stability threshold in high-performance internal-sin Nb_3Sn superconductors for high field magnets," *Superconducting Science and Technology, Rapid Communications*, Sep. 2004, submitted for publication.
[12] E. Barzi *et al.*, "Study of current carrying capability of Nb_3Sn cables in self-field using a SC current transformer," presented at the ASC 2004, Jacksonville, Fl., Oct. 3–8, 2004, paper 1LX06.
[13] G. Ambrosio *et al.*, "Critical current measurement of Nb_3Sn Rutherford-type cables for high field accelerator magnets," presented at the ASC 2004, Jacksonville, Fl., Oct. 3–8, 2004, paper 2LR03.
[14] V. V. Kashikhin and A. V. Zlobin, "Magnetic Instabilities in Nb_3Sn Strands,", FNAL Report: TD-03-032.
[15] L. Chiesa, "SM-02 Test Results,", LBNL SC-MAG 843.
[16] A. Lietzke, "Summary of SM-03 Quench Initiation and Propagation,", LBNL SC-MAG #844.
[17] K. Molnar and D. R. Dietderich, "Damage to Coil SC-06,", LBNL SC-MAG #808A.
[18] M. N. Wilson, *Superconducting Magnets*. Oxford: Oxford Univ. Press, 1983, ch. 7.
[19] C. King *et al.*, "Flux jump stability in Nb_3Sn tape," *IEEE Trans. Appl. Supercond.*, vol. 7, pp. 1524–1528, 1977.
[20] N. J. Simon, E. S. Drexler, and R. P. Reed, NIST Monograph 177, Properties of Copper and Copper Alloys at Cryogenic Temperatures.
[21] "International Standard Superconductivity—Part 2: Critical Current Measurement—DC Critical Current of Nb_3Sn Composite Superconductors.", CEI-IEC Report no. 61 788-2.
[22] T. Pyon and E. Gregory, "Nb_3Sn conductor for high energy physics and fusion applications," *IEEE Trans. Appl. Supercond.*, vol. 11, pp. 3688–3691, Mar. 2001.
[23] S. O. Prestemon *et al.*, "Design, fabrication, and test results of undulators using Nb_3Sn superconductor," presented at the ASC 2004, Jacksonville, Fl., Oct. 3–8, 2004, paper 1LW03.